JURNAL ELTEK
Vol. 24, No. 2, October 2026, pp. 102~110
p-ISSN: 1693 – 4024 | e-ISSN: 2355-0740
DOI: 10.33795/eltek.v24i2.10746

Annealing effects on single-phase E-I transformer performance under nonlinear loads

Slamet Nurhadi[1], Chandra Wiharya[2], Satria Luthfi Hermawan[3], Priya Surya Harijanto*[4], Bakti Indra Kurniawan[5], Divac Nabiel Akbar[6]

e-mail: slamet.nurhadi@polinema.ac.id, chandra.wiharya@polinema.ac.id, satrialthf@polinema.ac.id, priya.surya@polinema.ac.id, bakti@polinema.ac.id, nabiel@polinema.ac.id

[1,2,3,4,5,6]Department of Electrical Engineering, State Polytechnic of Malang, Indonesia

Article Information

Article History

Received July 28, 2026
Revised October 12, 2026
Published October 30, 2026

***Keywords*:**

Annealing
Core Loss
E-I Transformer
Harmonic Distortion
Voltage Regulation

ABSTRACT

Single-phase E-I transformers are widely used in power-conversion applications, including grid-connected flyback micro-inverters for solar photovoltaic systems, yet their performance often deteriorates due to high core loss and harmonic distortion generated by nonlinear loads. This study evaluated the effect of the annealing process on core loss, voltage regulation, energy efficiency, and voltage/current harmonic distortion of a single-phase E-I transformer under nonlinear loading. Three transformer samples were tested under no-load and nonlinear-load conditions (rectifier and inverter) before and after annealing at 180, 350, and 450 °C for 60 minutes, followed by harmonic-distortion measurement using a power logger on a flexible conveyor system and a single-phase induction motor. Annealing at 350 °C produced the most significant core-loss reduction, from 150.3 W to 110.6 W, while linear-load efficiency reached 97-98% and voltage regulation remained stable near 98%. Harmonic measurements showed voltage total harmonic distortion (THDv) of 5.8% on the flexible conveyor system and 5.6% on the induction motor without a variable speed drive, both below the 8% IEEE 519 limit, while individual current harmonic distortion (IHDi), current total harmonic distortion (THDi), and total demand distortion (TDD) also remained within the standard's safe margins. These findings indicate that medium-temperature annealing can improve the magnetic performance of the transformer core while keeping power quality within standard limits under nonlinear loading. The practical implication is that this annealing guideline can be adopted by small and medium-scale transformer manufacturers to improve energy efficiency without costly equipment investment.

Corresponding Author:
Priya Surya Harijanto, S.T., M.T.,
Department of Electrical Engineering,
State Polytechnic of Malang,
Jl. Soekarno-Hatta No. 9, Malang, East Java, Indonesia.
Email: priya.surya@polinema.ac.id

1. INTRODUCTION

Transformers are essential to every power-conversion process, from distribution networks to small devices such as battery chargers and UPS units. Single-phase E-I core transformers are especially common for their simple construction and low cost, including as the low-frequency stage inside flyback micro-inverters that connect solar PV panels to the grid, where they both step voltage and determine how efficiently renewable energy is delivered. Because Indonesia targets a gradual reduction in national energy intensity, component-level efficiency gains in transformers contribute meaningfully to that goal, making core heat treatment relevant both scientifically and industrially.

Small and medium-scale manufacturers chiefly struggle with high core loss at nominal voltage, which raises temperature, lowers reliability, and wastes energy. The problem compounds under nonlinear loads such as rectifiers and switching inverters, whose harmonic content adds core loss, degrades voltage regulation, and can overheat windings enough to force a derating of usable capacity. Uncertainty over annealing parameters, temperature, duration, and cooling rate, further prevents small manufacturers from standardizing core quality, underscoring the need for an evidence-based guideline that does not require expensive equipment.

Prior work links annealing temperature to core-loss reduction in silicon-iron: Zhang et al. cut hysteresis loss by over 30% annealing Fe-Si powder cores near 800 °C [1]; Du et al. linked post-annealing microstructure to leakage-flux-driven core loss [2]; Kühn et al. used multiphysics simulation to quantify grain-size effects on hysteresis and eddy-current loss [3]; and Zhou et al. and Yuan et al. achieved significant core-loss reduction annealing non-oriented silicon steel above 900 °C [4], [5]. These studies confirm that heat treatment improves magnetic properties, but mostly at very high temperatures under purely sinusoidal excitation, not the nonlinear loading that better represents field conditions.

The gap is a scarcity of studies combining medium-temperature annealing (below 500 °C) with realistic nonlinear loading and power-quality evaluation: most prior work stops at core-loss and efficiency, omitting THD, IHD, and TDD analysis, and rarely connects annealing results to real applications such as PV micro-inverters or conveyor systems within one integrated framework.

This study addresses that gap by annealing at 180, 350, and 450 °C for a uniform 60-minute hold, then evaluating core loss and voltage regulation under three realistic load scenarios, linear resistive, rectifier, and PWM inverter, and extending the evaluation with THDv, IHDi, THDi, and TDD measurements on a flexible conveyor system and a single-phase induction motor against IEEE 519 limits, giving a more complete picture of annealing's effect on both efficiency and power quality under real nonlinear operation.

This study therefore aims to: (1) analyze annealing's effect on E-I transformer core loss; (2) analyze voltage regulation of the annealed transformer under nonlinear loads; and (3) evaluate the potential capacity derating caused by overheating and harmonic distortion under nonlinear loading, together forming an annealing guideline that is both technically effective and economically viable for small and medium-scale manufacturers

2. RESEARCH METHOD

2.1. Material

The transformer core used Cold-Rolled Grain-Oriented (CRGO) Hi-B silicon-steel sheet (Nippon Steel, grade 23CG140; ≥99.5% Fe, 3.2% Si), chosen for its high permeability and low hysteresis loss typical of commercial distribution-transformer cores, keeping the results industry-representative. Sheets were cut to 50 mm × 20 mm E- and I-type laminations following IEC 60404-8-7, a shape producible with simple cutting equipment available to small industry, so the results can be adopted without precision machinery.

Primary and secondary windings used Class-H enameled copper wire (Elektrisola; AWG 24; ≥99.99% Cu purity; halogen-free polyimide coating), rated for continuous operation to 180 °C to accommodate the higher temperatures expected under nonlinear-load testing. The winding assembly was impregnated with Varnish Dolph 670H (polyester-imide, 45 ± 2% solids, rated to 180 °C) to mechanically bind the turns and improve insulation resistance against moisture and heat during repeated testing.

During post-fabrication cooling, residual lamination stress was minimized under ultra-high-purity argon (99.999%, Samator) at 5 L/min to prevent oxide-layer core loss. Annealing used a Carbolite GCF 11/23 electric furnace (11 L chamber, 1,200 °C maximum, two-zone PID control) for uniform chamber temperature.

Post-annealing core impedance was characterized with a Keysight E4980A LCR meter (20 Hz-2 MHz, 0.05% accuracy) at 100 Hz and 1 kHz to match operating frequency. AC power loss was measured with a Yokogawa WT310E power analyzer (0.1% of reading + 0.05% of range) and a Mangores nichrome resistor bank for linear loading; nonlinear loads used a Vishay VS-GBPC3508 diode-bridge rectifier and a prototype inverter built around an Infineon IPW60R099 MOSFET.

Harmonic measurements used a Fluke 1736 power logger (spectrum to the 49th order) at the point of common coupling of the conveyor system and induction motor, while post-annealing temperature was logged with an Omega 5SRTC Type-K thermocouple via a 16-channel NI 9213 data logger.



Figure 1. Prototype of the single-phase E-I transformer with core laminations that had undergone the annealing process

2.2. Methods

This study followed the research flow diagram in Figure 2: preparation, pre-annealing baseline testing, annealing, repeated post-annealing testing, data analysis, and conclusion. The design was a comparative experiment with four treatment groups, one non-annealed control and three annealed at 180, 350, and 450 °C.

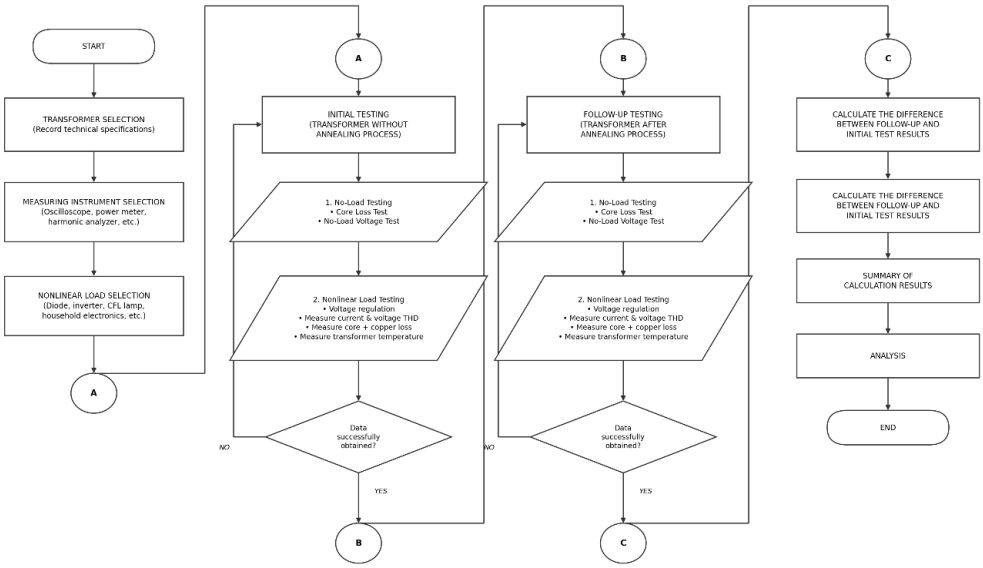


Figure 2. Research flow diagram

The preparation stage selected the single-phase E-I transformer as the research object, documented its voltage, power, core type, and winding specifications, and prepared all test instruments, oscilloscope, power analyzer, harmonic analyzer, and rectifier/inverter nonlinear-load circuits, following validated material- and component-testing approaches [6].

Baseline (pre-annealing) testing established no-load core loss and no-load voltage using the single-strip Epstein method (flux density 1 T at 50 Hz; voltage and current logged at 100 kS/s), then repeated under non-sinusoidal load to record baseline harmonic distortion, total power loss, and operating temperature as a reference point for later comparison.

Insulation integrity was checked beforehand with a megohmmeter across the primary-ground, secondary-ground, and primary-secondary paths at 1 kV; results appear with the transformer characterization data in Section 3.1 (Table 1).

AC core loss was characterized with the same Epstein setup (1 T, 50 Hz, 100 kS/s). Under resistive load, a nichrome-wire bank was connected to the secondary up to the 2.1 A rated current, with efficiency computed per IEC 60076-1.

The rectifier scenario used a full-wave diode bridge with a 2 mF smoothing capacitor, analyzed by 1024-point FFT for total harmonic distortion; the inverter scenario used a 20 kHz full-bridge MOSFET topology at duty cycles of 0.4 and 0.8 to approximate line-interactive UPS operation, with core surface temperature held below the 90 °C varnish limit.

The annealing stage itself followed the heating, hold, and controlled-cooling profile detailed in Section 2.2.1.

Because the previous year's study had identified 350 °C as optimal, the current-year testing re-validated that finding and extended it to more complex nonlinear loading. Post-annealing testing repeated the no-load core-loss, harmonic-distortion, power-loss, voltage-regulation, and operating-temperature measurements under nonlinear load for direct comparison against the pre-treatment baseline.

As an extension, harmonic analysis was performed on an actual installation, a flexible conveyor system and a single-phase induction motor fed from the utility grid through the point of common coupling at an automatic transfer switch output. A power logger recorded THDv, IHDi, THDi, and TDD, compared against IEEE 519-2014/2019 limits [8].

THDi and TDD followed the standard IEEE 519 formulation for sub-1 kV systems [8]: the root-sum-square of each harmonic's RMS current, divided by the fundamental current (THDi) or by the maximum demand load current (TDD), as defined in Equations (3) and (4) in Section 3.6.

All instruments were calibrated under SNI ISO/IEC 17025-2017 at the Instrumentation Laboratory of State Polytechnic of Malang, with measurement uncertainty calculated by the root-sum-square method (BIPM GUM 1995). Where multiple loading points existed within a transformer sample (Sections 3.2-3.3), the Shapiro-Wilk test ($\alpha = 0.05$) checked normality of the within-sample efficiency and voltage-regulation distributions before descriptive comparison. For the annealing-temperature screening in Section 3.4 (Table 7), however, each condition (control, 180, 350, 450 °C) has only one core-loss measurement (n = 1); a single observation per group cannot support Shapiro-Wilk, paired t-test, or ANOVA, all of which need at least two replicates to estimate within-group variance. That comparison is therefore reported descriptively, as point-value differences, with replicated trials flagged as necessary future work (Section 4).

The final stage compared post-annealing results against the pre-annealing baseline and applicable standards, quantifying differences in core loss, voltage regulation, efficiency, and temperature rise and checking THD/TDD compliance with IEEE 519, to recommend the most suitable annealing temperature for small- and medium-scale manufacturing.

A note on sample labeling avoids ambiguity between two naming schemes used later in this paper. "Transformer 1," "Transformer 2," and "Transformer 3" (Sections 3.2-3.3) are three physically distinct units built and tested in the current study year for linear- and nonlinear-load characterization, all annealed at 350 °C, the condition identified as optimal during temperature screening. "TR1-TR4," by contrast, denote the four annealing-temperature conditions used in that screening stage (Table 7): TR1 is the non-annealed control, and TR2-TR4 correspond to 180, 350, and 450 °C, carried forward from the previous year's study [6]. The two schemes describe different aspects of the design and should not be cross-referenced interchangeably.

2.2.1 Annealing Procedure

Each core was heated at 5 °C/min to its target temperature, held for 60 minutes, then cooled naturally inside the closed furnace to 80 °C before exposure to ambient air, per ASTM A912-20 Section 5.2, avoiding rapid cooling that could cause plastic distortion or lamination micro-cracking [7].

2.2.2 Efficiency and Voltage Regulation

Transformer quality was assessed jointly through allowable temperature rise and voltage regulation, without sacrificing compactness. Secondary-side capacitance and leakage inductance were both assumed negligible given the transformer's low secondary voltage and frequency and its winding geometry. Voltage regulation is expressed as

$$\alpha = [V_0(N.L.) - V_0(F.L.)] / V_0(F.L.) \times 100\% \quad (1)$$

where α is the voltage regulation (%), V_0(N.L.) is the no-load secondary voltage (V), and V_0(F.L.) is the full-load secondary voltage (V). Efficiency, the ratio of output to input electrical power, is expressed as

$$\eta = (P_o / P_i) \times 100\% = [P_o / (P_o + \Sigma losses)] \times 100\% \quad (2)$$

where η is efficiency (%), P_o is output power (W), P_i is input power (W), and Σlosses is the sum of core loss and copper loss (W).

3. RESULTS AND DISCUSSION

3.1. Insulation Resistance Test and Transformer Characteristics

Insulation-resistance testing on all three samples showed no leakage or discharge on any of the three test paths at 1 kV (Table 1), confirming suitability for further load testing.

Table 1. Insulation resistance test results

No.	Megger Voltage (kV)	Parameter	Result
1	1	Primary-Ground	No leakage current, no discharge
2	1	Secondary-Ground	No leakage current, no discharge
3	1	Primary-Secondary	No leakage current, no discharge

The specifications of the annealed transformer used in the characterization test are shown in Table 2.

Table 2. E-I transformer specification

Po (Watt)	Vin (Volt)	Vout (Volt)	f (Hz)	η (%)
350	6	220	50	95

Three samples were tested: a non-annealed control and units annealed at 350 °C, the condition shown by the prior study stage to yield the greatest core-loss reduction.

3.2. Performance Under Linear Load (Nichrome Wire)

Each transformer was loaded with a 2 mm² nichrome-wire bank (0.85 Ω) up to rated current. Transformer 1 (Table 3) shows voltage regulation stable near 98%, while efficiency dipped to 79.9% at intermediate loading before recovering to 97.7% near rated current.

Table 3. Loading test data for Transformer 1 with nichrome wire

Vp (V)	Ip (A)	Vs (V)	Is (A)	Pp (W)	Ps (W)	PFp	PFs	Efficiency (%)	V.Reg (%)
220	0.4	5.86	9.8	59	56.85	0.67	0.99	96.36	98.34
220	0.6	5.81	14.3	93.7	82.25	0.71	0.99	87.78	98.36
220	0.9	5.78	20.7	156.4	140.45	0.79	0.99	89.80	98.37
220	1.0	5.62	25.9	180.4	144.1	0.82	0.99	79.88	98.45
220	1.04	5.58	31.3	201.3	172.91	0.88	0.99	85.90	98.46
220	1.09	5.52	39.7	220.6	216.95	0.92	0.99	98.35	98.49
220	1.1	5.37	42.2	229.9	224.35	0.95	0.99	97.59	98.56
220	1.3	5.29	51.2	274.6	268.14	0.96	0.99	97.65	98.60

Transformer 2 (Table 4) and Transformer 3 (Table 5) show a similar pattern, with efficiency ranging 80.5-91.5% and 74-88.6% respectively and voltage regulation again near 98% throughout, indicating that design flux density, not just core-loss magnitude, governs the optimal loading point.

Table 4. Loading test data for Transformer 2 with nichrome wire

Vp (V)	Ip (A)	Vs (V)	Is (A)	Pp (W)	Ps (W)	PFp	PFs	Efficiency (%)	V.Reg (%)
220	0.7	5.91	11.7	88	78.95	0.55	0.99	89.72	98.31
220	0.9	5.83	18.9	135.6	109.09	0.71	0.99	80.45	98.35
220	0.9	5.78	27.4	173.8	156.79	0.79	0.99	90.21	98.37
220	1.06	5.71	32.8	207.5	185.42	0.89	0.99	89.36	98.40
220	1.09	5.65	34.2	209.1	191.3	0.88	0.99	91.49	98.43
220	1.3	5.59	42.9	263.1	237.41	0.92	0.99	90.24	98.46
220	1.5	5.52	50.4	302.9	275.43	0.93	0.99	90.93	98.49
220	1.8	5.31	61.5	372.24	329.76	0.94	0.99	88.59	98.59

Table 5. Loading test data for Transformer 3 with nichrome wire

Vp (V)	Ip (A)	Vs (V)	Is (A)	Pp (W)	Ps (W)	PFp	PFs	Efficiency (%)	V.Reg (%)
220	0.8	5.99	12.2	90.3	73.56	0.51	0.99	81.46	98.28
220	1.0	5.87	20.7	156.2	120.29	0.71	0.99	77.01	98.33
220	1.03	5.81	24.1	179	138.62	0.79	0.99	77.44	98.36
220	1.09	5.78	27.4	208.6	156.79	0.87	0.99	75.16	98.37
220	1.1	5.67	30.9	213	173.45	0.88	0.99	81.43	98.42
220	1.3	5.58	42.2	263.1	233.12	0.92	0.99	88.61	98.46
220	1.6	5.46	46.1	320.3	249.19	0.91	0.99	77.80	98.52
220	1.8	5.37	61.8	350.4	290.73	0.94	0.99	82.97	98.56

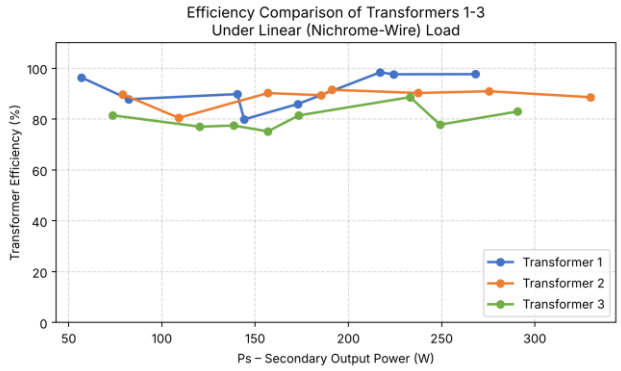


Figure 3. Efficiency comparison, linear load

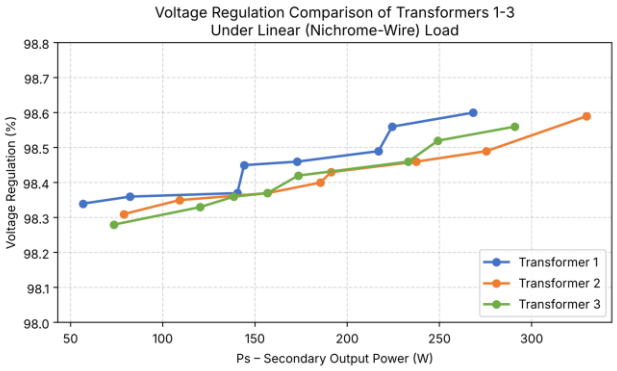


Figure 4. Voltage regulation comparison, linear load

3.3. Performance Under Nonlinear Load (Rectifier and Inverter)

Adding a diode-bridge rectifier consistently lowered efficiency versus the linear condition, especially at high loading: Transformer 1 dropped to about 51% while Transformer 3 stayed more stable at 74-91%. Voltage regulation remained near 98% for all samples, indicating the decline came from harmonic-related loss rather than voltage instability.

Under PWM inverter loading, Transformer 1 efficiency instead rose monotonically with load current, from 57.9% to 87.6% near rated current (Table 6), unlike the linear and rectified cases, indicating that fixed core loss becomes a proportionally smaller share of output power at high switching frequency as loading increases.

Table 6. Transformer 1 characteristics under inverter load

Vp (V)	Ip (A)	Vs (V)	Is (A)	Pp (W)	Ps (W)	η (%)
6.79	28	220	0.5	190.12	110	57.86
6.65	58	220	1.32	385.7	290.4	75.29
6.4	81	220	1.87	518.4	411.4	79.36
6.2	83	220	2.05	514.6	451	87.64

3.4. Effect of Annealing Temperature on Core Loss

Table 7 summarizes core loss across annealing temperatures. Against the control (150.3 W), 180 °C gave only a marginal reduction (148.2 W), while 350 °C produced the largest drop, to 110.6 W (≈26%). At 450 °C, core loss rose again to 137.1 W but stayed below control. As noted in Section 2.2, this comparison is descriptive (n = 1 per condition).

Table 7. Core loss versus annealing temperature

No.	Unit	Annealing Temperature (°C)	Core Loss (W)
1	TR1	No annealing (control)	150.3
2	TR2	180	148.2
3	TR3	350	110.6
4	TR4	450	137.1

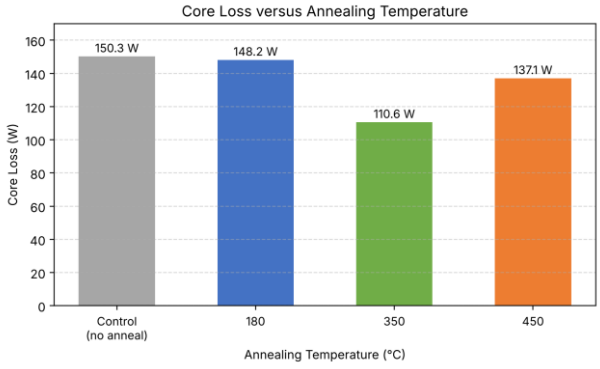


Figure 5. Core loss versus annealing temperature

This non-monotonic pattern fits a thermally driven residual-stress-relaxation mechanism optimal at medium temperature: below 350 °C relief is incomplete, while above it grain growth and renewed thermal stress offset the benefit. This is directionally consistent with Du et al. and Zhang et al., who linked core-loss reduction to improved grain orientation and stress relief [1], [2], though at substantially higher temperatures (above 600 °C), confirming that the medium-temperature window found here is more economically relevant for furnace-limited small industry.

3.5. Harmonic Analysis of the Flexible Conveyor System

At the automatic transfer switch's point of common coupling supplying the unloaded conveyor system, average THDv was 5.8%, dominated by the 3rd, 5th, and 7th harmonics (Figure 6). Current harmonics were not detected since no load current was drawn yet. The 5.8% THDv is below the IEEE 519-2014 8% limit for sub-1 kV systems, so voltage quality met the standard.

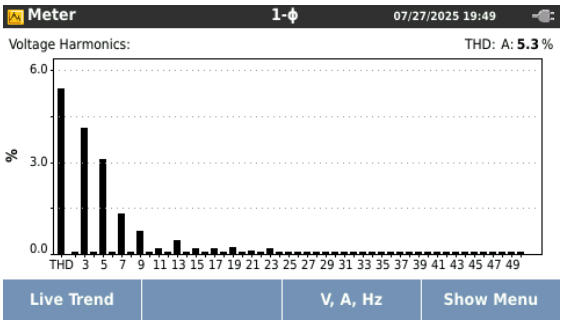


Figure 6. THDv spectrum – conveyor system

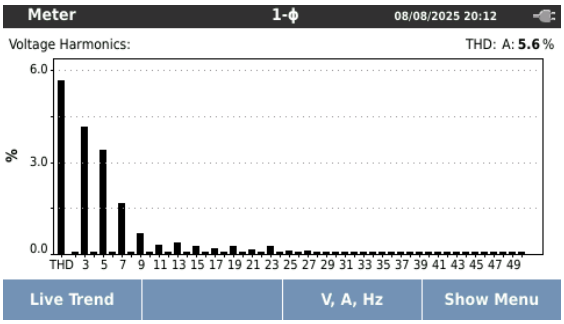


Figure 7. THDv spectrum – motor without VSD

3.6. Harmonic Analysis of the Single-Phase Induction Motor Without a VSD

With the induction motor connected directly to the grid without a VSD or the conveyor, average THDv was 5.6%, dominated by the 3rd order (Figure 7), also below the 8% IEEE 519-2014 limit. The current harmonic spectrum for each order is summarized in Table 8.

Table 8. IHDi values under the motor-without-VSD condition

Order	RMS Value (A)	IHD (%)
1	1.01	–
3	0.06	0.06
5	0.06	0.06
7	0.03	0.03
9	0.01	0.01
11	0	0
... up to 49	0	0.00

The highest IHDi values, 0.06% at the 3rd and 5th orders, are well below the 5% per-order IEEE 519-2014 limit. THDi was calculated following Equation (3):

$$THDi = \sqrt{(\Sigma_{h=2..hmax} M_h^2)} / M_1 \times 100\% \quad (3)$$

With a squared-IHDi sum of 0.01 and fundamental current M_1 = 1.01 A, THDi is 0.090%, well below the 8% IEEE 519-2014 limit. TDD was calculated following Equation (4):

$$TDD = \sqrt{(\Sigma_{h=2..hmax} I_n^2)} / I_L \times 100\% \quad (4)$$

With maximum demand current I_l = 1.5 A during motor starting, TDD = 0.60%, well under the 5.0% IEEE 519-2019 limit applicable when I_l is below 20 [8].

Overall, harmonic results on both the conveyor system and induction motor remained within IEEE 519 limits before and after the annealed transformer entered service, supporting that improved core magnetics does not introduce new power-quality risk and instead enables more efficient operation without compromising harmonic compliance. Full-load THD on the conveyor system after annealing was not captured in this campaign and is identified as future work (Section 4).

4. CONCLUSION

This study addressed high core loss, voltage instability, and harmonic-related derating in single-phase E-I transformers under nonlinear loads, relevant to small and medium manufacturers and to grid-connected PV micro-inverters. Because core loss alone accounts for a substantial share of total transformer losses, a process-level improvement such as annealing carries a proportionally large effect on national-scale energy efficiency.

Annealing at 350 °C for 60 minutes produced the greatest core-loss reduction (150.3 W to 110.6 W) while sustaining 97-98% linear-load efficiency and ≈98% voltage regulation. Lower (180 °C) and higher (450 °C) temperatures gave smaller or partially reversed gains, marking a turning point beyond which grain growth and renewed thermal stress outweigh further stress relief. Under nonlinear loading, efficiency fell with rectifier loads but rose monotonically with inverter loads, and harmonic measurements on the conveyor system and induction motor gave THDv of 5.8% and 5.6%, with IHDi, THDi, and TDD all within IEEE 519 limits.

These results agree with Zhang et al. and Du et al., who linked annealing-induced core-loss reduction to improved grain orientation and stress relief, but diverge from Zhou et al. and Yuan et al., whose gains came above 900 °C: this study shows a much lower, medium-temperature window delivers a directionally comparable benefit, supporting the general high-temperature mechanism while contradicting the assumption that high temperatures are necessary, at least within the range examined here.

Future work should: (1) test additional temperatures between 250 and 500 °C with replicated trials so the Shapiro-Wilk, paired t-test, and ANOVA procedures of Section 2.2 can be meaningfully applied; (2) measure harmonic distortion directly at the transformer terminals under full nonlinear loading, including the full-load conveyor-system THD noted in Section 3.6, to isolate the transformer's own contribution; (3) evaluate annealing duration and cooling rate independently of peak temperature; and (4) validate the approach on non-oriented and amorphous core laminations to test how broadly these findings generalize.

5. ACKNOWLEDGMENTS

This research was funded by the DIPA Fund of State Polytechnic of Malang, Number SP DIPA-139.03.2.693474/2025. The authors thank the Power Electronics and Electric Motor Control Laboratory of State Polytechnic of Malang for its testing facility support.

6. REFERENCES

[1] Z. Zhang et al., "Effects of Annealing Temperature and Compaction Pressure on Magnetic Properties of Fe–Si Powder Cores Fabricated by an Improved Bluing Method," J. Supercond. Nov. Magn., vol. 31, no. 5, pp. 1507-1513, May 2018, doi: 10.1007/S10948-017-4358-0.

[2] Y. Du, W. Zheng, and J. Zhang, "Modeling and Analysis of Leakage Flux and Iron Loss Inside Silicon Steel Laminations," Int. J. Energy Power Eng., vol. 5, no. 1, pp. 48-52, 2016, doi: 10.11648/J.IJEPE.S.2016050101.17.

[3] P. Kühn, Y. Yang, G. Chen, S. N. Foster, H. Egger, and B.-X. Xu, "Multiphysics simulations of microstructure influence on hysteresis and eddy current losses of electrical steel," arXiv preprint, Feb. 2025. [Online]. Available: https://arxiv.org/abs/2502.01559v1

[4] C. Zhou, S. Luan, J. Qiao, and H. Wang, "Effect of Normalizing Temperature on Microstructure, Texture and Magnetic Properties of Non-Oriented Silicon Steel," Metals, vol. 15, no. 2, p. 217, Feb. 2025, doi: 10.3390/MET15020217.

[5] J. Yuan et al., "Effect of annealing time on microstructure and properties of high-strength non-oriented silicon steel with Nb addition," J. Mater. Res. Technol., vol. 36, pp. 3756-3772, May 2025, doi: 10.1016/J.JMRT.2025.04.056.

[6] S. Nurhadi, A. D. Nofvowan, S. L. Hermawan, and B. S. Gumilang, "Pengaruh Variasi Proses Annealing pada Performa Core Losses Trafo 1 Fasa E-I," ELPOSYS: J. Sistem Kelistrikan, vol. 12, no. 2, pp. 138-143, Jun. 2025.

[7] ASTM International, ASTM A912-20: Standard Practice for Heat Treatment of Electrical Steel, ASTM International, West Conshohocken, PA, 2020.

[8] IEEE Std 519-2014/2019, IEEE Recommended Practice and Requirements for Harmonic Control in Electric Power Systems, Institute of Electrical and Electronics Engineers, New York, 2014/2019.

[9] B. Mitra, A. Singhal, S. Kundu, and J. P. Ogle, "Analyzing Distribution Transformer Degradation with Increased Power Electronic Loads," in Proc. 2023 IEEE PES ISGT, Oct. 2022, doi: 10.1109/ISGT51731.2023.10066387.

[10] M. H. Mohd Wazir et al., "Harmonics Assessment of Distribution Transformer with Photovoltaic Integration and Unbalanced Loads," Elektrika J. Electr. Eng., vol. 23, no. 1, pp. 81-87, Apr. 2024, doi: 10.11113/ELEKTRIKA.V23N1.504.

[11] P. Osinski and P. Witczak, "Analysis of Core Losses in Transformer Working at Static Var Compensator," Energies, vol. 16, no. 12, p. 4584, Jun. 2023, doi: 10.3390/EN16124584.

[12] X. Ma, R. Jia, C. Liang, H. Du, X. Dong, and M. Ding, "Study of Transformer Harmonic Loss Characteristic in Distribution Network Based on Field-Circuit Coupling Method," Sustainability, vol. 14, no. 20, p. 12975, Oct. 2022, doi: 10.3390/SU142012975.
[13] I. Ziger, B. Trkulja, and Ž. Štih, "Determination of Core Losses in Open-Core Power Voltage Transformers," IEEE Access, vol. 6, pp. 29426-29435, 2018, doi: 10.1109/ACCESS.2018.2838446.